Acta Mechanica 132, 113–127 (1999)

ACTA MECHANICA

Non-Darcian effects on double diffusive convection in a sparsely packed porous medium

I. S. Shivakumara and **R. Sumithra,** Bangalore, India

(Received July 16, 1997; revised October 16, 1997)

Summary. The linear and non-linear stability of double diffusive convection in a sparsely packed porous layer is studied using the Brinkman model. In the case of linear theory conditions for both simple and Hopf bifurcations are obtained. It is found that Hopf bifurcation always occurs at a lower value of the Rayleigh number than one obtained for simple bifurcation and noted that an increase in the value of viscosity ratio is to delay the onset of convection. Non-linear theory is studied in terms of a simplified model, which is exact to second order in the amplitude of the motion, and also using modified perturbation theory with the help of self-adjoint operator technique. It is observed that steady solutions may be either subcritical or supercritical depending on the choice of physical parameters. Nusselt numbers are calculated for various values of physical parameters and representative streamlines, isotherms and isohalines are presented.

1 Introduction

Double diffusive convection is a type of instability that occurs in a fluid which possesses two density-altering constituents with differing molecular diffusivities, such as certain motions in the oceans and some lakes where the two properties are heat and salt. Copious literature is available on double diffusive convection in classical fluids and reviewed extensively (see Huppert and Turner [1]), whereas its counterpart in porous media has received comparatively little attention in spite of its wide applications in geothermal reservoir, moisture migration in thermal insulations and stored grain, underground spreading of chemical pollutants, waste and fertiliser migration in saturated soil and so on.

Nield [2], Rubin [3], Lightfoot and Taunton [4] and Rudraiah et al. [5] have studied double diffusive convection in porous media by considering the Darcy flow model which is relevant to densely packed, low permeability porous media. However, experiments conducted with several combinations of solids and fluids covering wide ranges of governing parameters indicate that most of the experimental data do not agree with the theoretical predictions based on the Darcy flow model. Hence, non-Darcy effects on double diffusive convection in porous media have received a great deal of attention in recent years. Poulikakos [6] has used the Brinkman extended Darcy flow model for the problem to investigate the linear stability analysis. Nevertheless, the variation in the ratio of effective viscosity of the porous medium to the fluid dynamic viscosity and transition from oscillatory to direct instability are not studied. Recently Givler and Altobelli [7] have demonstrated that for high permeability porous media the effective viscosity is about ten times the fluid viscosity. Therefore, the effect of viscosities on the stability analysis is of practical interest. One of the aims of this paper is to study these aspects.

It is known that, when the solute gradient is very stable, steady finite amplitude convective motions exist at a value of the Rayleigh number smaller than the value required for the onset of infinitesimal perturbations. In such cases the linear theory fails to give information about the stability of these finite amplitude solutions. Hence, the study of nonlinear double diffusive convection naturally arises, and the chief aim of the present work is to study the same. For this purpose, we consider a two-dimensional double diffusive convection in a porous layer and contruct a fifth order system of ordinary differential equations which possesses both periodic and steady solutions and allows subcritical convection (for details see Da Costa et al. [8] and references therein). The condition for the existence of steady finite amplitude solutions is obtained from this system. Finite amplitude steady solutions are also obtained using modified perturbation theory for the full two-dimensional problem with the help of self-adjoint operator technique. It is shown that the results obtained from the truncated system are identical to those for the full two-dimensional problem to second order. Only steady finite amplitude solutions are discussed, and work is in progress to consider time-dependent finite amplitude motions.

2 The model

We consider a two-dimensional double diffusive convection in a horizontally unbounded fluid saturated porous layer of thickness d in which the density ϱ depends on two different stratifying agencies (solute concentration and temperature). The model is based on the assumption of a Boussinesq fluid with all physical properties being treated as constants except for density in the buoyancy term, where ϱ is taken as

$$\varrho = \varrho_0\{1 - \alpha_t(T - T_0) + \alpha(S - S_0)\}.$$

Here, T is the temperature, S is the solute concentration, α_t is the thermal expansion co-efficient, α_s is the solute analog of α_t, and ϱ_0 is a reference fluid density. We introduce a stream function ψ so that the velocity

$$\vec{q} = \left(\frac{\partial\psi}{\partial z}, 0, -\frac{\partial\psi}{\partial x}\right).$$

It is assumed that at the quiescent state both the temperature and solute concentration vary linearly across the depth with values $T_0 + \Delta T$, $S_0 + \Delta S$ and T_0, S_0 at the bottom and top free surfaces, respectively.

We scale length, time, temperature, solute concentration and velocity by d, $d^2M/\varkappa$, ΔT, ΔS and $\varkappa/d$, respectively. The dimensionless nonlinear perturbation equations following Nield and Bejan [9] can be written as

$$\left(\frac{\lambda}{P_r}\frac{\partial}{\partial t} + \frac{1}{D_a} - \Lambda\nabla^2\right)\nabla^2\psi = -R\,\frac{\partial\theta}{\partial x} + R_s\frac{\partial\Sigma}{\partial x} + \frac{1}{P_r}\,J(\psi, \nabla^2\psi), \tag{1}$$

$$\left(\frac{\partial}{\partial t} - \nabla^2\right)\theta = -\frac{\partial\psi}{\partial x} + J(\psi, \theta), \tag{2}$$

$$\left(\lambda\,\frac{\partial}{\partial t} - \tau\nabla^2\right)\Sigma = -\frac{\partial\psi}{\partial x} + J(\psi, \Sigma), \tag{3}$$

where θ and Σ are dimensionless temperature and solute concentration, $R = \alpha_t g\Delta T d^3/\nu\varkappa$, $R_s = \alpha_s g\Delta S d^3/\nu\varkappa$, $D_a = k/d^2$ and $P_r = \varphi^2\,\nu/\varkappa$ are the thermal Rayleigh, solute Rayleigh,

Darcy and effective Prandtl numbers, respectively, $\lambda = \varphi/M$ and $M = \varphi + (1-\varphi)\gamma$ are the non-dimensional groups, while $\Lambda = \widetilde{\mu}/\mu$, $\tau = \varkappa_s/\varkappa$, $\gamma = (\varrho C)_s/(\varrho C)_f$ are the ratios of viscosities, diffusivities and heat capacities, respectively. Here $\varkappa$, $\varkappa_s$, ν are the thermal, solutal and viscous diffusivities while k is the permeability of the porous medium, φ is the porosity, J is the Jacobian, $\widetilde{\mu}$ is the effective viscosity of the medium and μ is the fluid viscosity. In general $\widetilde{\mu}$ is not equal to μ and hence we have taken the ratio of these two viscosities as an independent parameter in the present study to know its true effect on the stability of the system.
The boundary conditions are

$$\psi = \frac{\partial^2 \psi}{\partial z^2} = \theta = \Sigma = 0 \qquad \text{at} \qquad z = 0,\ 1. \tag{4}$$

The non-linear boundary value problem given by Eqs. (1)–(4) admits the solution

$$\psi = \frac{2\sqrt{2}}{\alpha}\, K A(t^*) \sin \alpha x \sin \pi z, \tag{5}$$

$$\theta = \frac{2\sqrt{2}}{K}\, B(t^*) \cos \alpha x \sin \pi z - \frac{C(t^*)}{\pi} \sin 2\pi z, \tag{6}$$

$$\Sigma = \frac{2\sqrt{2}}{K}\, D(t^*) \cos \alpha x \sin \pi z - \frac{E(t^*)}{\pi} \sin 2\pi z \tag{7}$$

provided [A, B, C, D, E] satisfies

$$\dot{A} = -\frac{P_r}{\lambda}\left(\eta A + \frac{R\alpha^2}{K^6} B - \frac{R_s \alpha^2}{K^6} D\right), \tag{8.1}$$

$$\dot{B} = A(C-1) - B, \tag{8.2}$$

$$\dot{C} = -\varpi(AB + C), \tag{8.3}$$

$$\dot{D} = \frac{A(E-1)}{\lambda} - \frac{\tau D}{\lambda}, \tag{8.4}$$

$$\dot{E} = -\varpi(AD + \tau E), \tag{8.5}$$

where $t^* = K^2 t$, $K^2 = \pi^2 + \alpha^2$ is the total wavenumber, $\varpi = 4\pi^2/K^2$, $\eta = \Lambda + 1/D_\alpha K^2$ and the dot above the quantities denotes the differentiation with respect to t^*. These equations possess two significant properties. First, the divergence of the flow in a five dimensional phase space,

$$\frac{\partial \dot{A}}{\partial A} + \frac{\partial \dot{B}}{\partial B} + \frac{\partial \dot{C}}{\partial C} + \frac{\partial \dot{D}}{\partial D} + \frac{\partial \dot{E}}{\partial E} = -\left(\frac{P_r \eta}{\lambda} + 1 + \varpi + \frac{\tau}{\lambda} + \varpi\frac{\tau}{\lambda}\right)$$

is always negative and so the solutions are attracted to a set of measure zero in the phase space and this may be a fixed point, a limit cycle or a strange attractor. Second, the equations have an important symmetry, for they are invariant under the transformation $(A,\ B,\ C,\ D,\ E) \to (-A,\ -B,\ C,\ -D,\ E)$.

2.1 Bifurcations from the static solution

Equations (8.1)–(8.5) admit the trivial solution $A = B = C = D = E = 0$ that corresponds to pure conduction of heat and solute with no fluid motion present. The linear stability properties of this static solution may be obtained from Eqs. (8.1)–(8.5) upon neglecting all non-linear terms and seeking solutions of the form $e^{\sigma t^*}$, where σ is the growth rate. Equations

(8.1), (8.2) and (8.4) finally yield the dispersion relation

$$\left(\frac{\lambda}{P_r}\sigma + \frac{1}{D_a} + \Lambda K^2\right)(\sigma + K^2)(\lambda\sigma + \tau K^2) K^2 = R\alpha^2(\lambda\sigma + \tau K^2) - R_s\,\alpha^2(\sigma + K^2). \tag{9}$$

We see that Eq. (9) coincides with that of Veronis [10] as $D_a \to \infty$, $\Lambda = 1$ and $\varphi = 1$ (classical viscous case) and Rudraiah et al. [5] as $D_a \to 0$ (Darcy case) with appropriate scaling, suggesting that the results obtained from the truncated model problem will be identical to those for the full two dimensional problem.

The onset of instability can be examined by setting the real part of σ equal to zero so that $\sigma = i\omega$. Taking R as a free parameter (assuming α^2, τ, λ, Pr, D_a, Λ and R_s as given) and clearing the complex quantities from the denominator, Eq. (9) can be re-written in the form

$$R = R_s\,\frac{\omega^2\lambda + \tau K^4}{\omega^2\lambda^2 + \tau^2 K^4} + \frac{K^6}{\alpha^2}\eta - \frac{\lambda K^2}{P_r\alpha^2}\omega^2 + i\omega K^2 N, \tag{10}$$

where

$$N = \frac{R_s(\tau - \lambda)}{\omega^2\lambda^2 + \tau^2 K^4} + \frac{K^2}{\alpha^2}\left(\eta + \frac{\lambda}{P_r}\right).$$

Since R is a physical quantity, Eq. (10) implies either $\omega = 0$ or $N = 0$ and accordingly we can obtain the conditions for the occurrence of simple and Hopf bifurations.

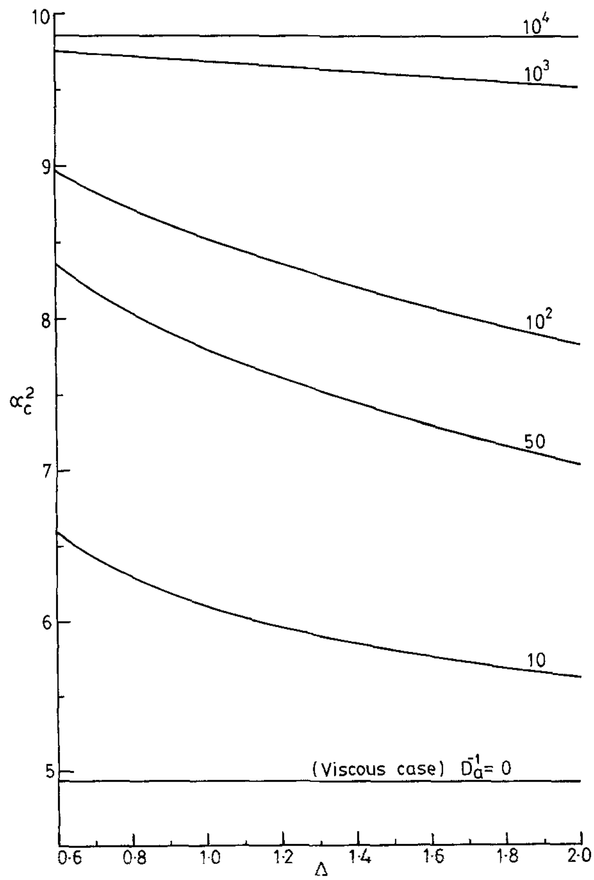

Fig. 1. Variation of critical wavenumber with Λ for various values of D_a^{-1}

2.2 Simple bifurcation

Simple bifurcation occurs at $R = R^d$, where

$$R^d = \frac{R_s}{\tau} + \frac{K^6}{\alpha^2}\,\eta. \tag{11}$$

R^d attains its minimum value, $R^d_{\min}$ when $\alpha^2 = {\alpha_c}^2$, where

$${\alpha_c}^2 = \frac{-\left(\pi^2 \Lambda + \frac{1}{D_a}\right) + \sqrt{\left(\pi^2 \Lambda + \frac{1}{D_a}\right)\left(9\pi^2 \Lambda + \frac{1}{D_a}\right)}}{4\Lambda}. \tag{12}$$

We see that the critical wavenumber is independent of R_s and τ but depends on the viscosity ratio and Darcy number. The critical wavenumbers obtained for different values of ${D_a}^{-1}$ and Λ are shown graphically in Fig. 1. For a fixed value of ${D_a}^{-1}$, increasing Λ decreases the critical horizontal wavenumber. However in the classical viscous and Darcy flow limits (i.e., ${D_a}^{-1} \ll 1$ and ${D_a}^{-1} \gg 1$ respectively) the dependence of Λ on ${\alpha_c}^2$ is not noticeable as expected. In these two limiting cases ${\alpha_c}^2$ attains the value $\pi^2/2$ and π^2, respectively. Also for a fixed value of Λ, increase in ${D_a}^{-1}$ is to increase the value of ${\alpha_c}^2$.

2.3 Hopf bifurcation ($\omega \neq 0,\ N = 0$)

There is a Hopf bifurcation from the static solution at $R = R^o$, where

$$R^o = \left(\frac{R_s}{P_r\eta + \lambda} + \frac{K^6(\tau + \lambda)}{P_r\alpha^2}\right)\frac{P_r\eta + \tau}{\lambda}, \tag{13}$$

provided that

$$\omega^2 = \frac{R_s(\lambda - \tau)\,\alpha^2}{K^2\lambda^2\left(\eta + \frac{\lambda}{P_r}\right)} - \frac{K^4\tau^2}{\lambda^2} = \frac{P_r\tau\alpha^2(R^d - R^o)}{K^2\lambda(P_r\eta + \lambda + \tau)} \tag{14}$$

is positive. Thus, from Eq. (14) it is clear that, if a Hopf bifurcation is possible at all, it always occurs at a lower value of the thermal Rayleigh number than that of the simple bifurcation. Since $\omega^2 > 0$, a necessary condition for the existence of a Hopf bifurcation is

$$\tau < \lambda, \qquad R_s > {R_s}^* = \frac{K^6\eta}{\alpha^2}\left(\frac{\tau^2}{\lambda - \tau}\right)\left(1 + \frac{\lambda}{P_r\eta}\right).$$

R^o attains its minimum value, $R^o_{\min}$ at $\alpha^2 = {\alpha_c}^2$, ${\alpha_c}^2$ being the root of the polynomial

$$a_5Y^5 + a_4Y^4 + a_3Y^3 + a_2Y^2 + a_1Y + a_0 = 0, \tag{15}$$

where

$$a_5 = 2D_a\left(\Lambda + \frac{\tau}{P_r}\right)\left(\Lambda + \frac{\lambda}{P_r}\right)^2,$$

$$a_4 = \left[\left\{4 - 3\pi^2 D_a\left(\Lambda + \frac{\lambda}{P_r}\right)\right\}\left(\Lambda + \frac{\tau}{P_r}\right) + \left(\Lambda + \frac{\lambda}{P_r}\right)\right]\left(\Lambda + \frac{\lambda}{P_r}\right),$$

$$a_3 = \frac{2}{D_a}\left\{1 - 3\pi^2 D_a\left(\Lambda + \frac{\lambda}{P_r}\right)\right\}\left(\Lambda + \frac{\tau}{P_r}\right) + \frac{2}{D_a}\left\{1 - \pi^2 D_a\left(\Lambda + \frac{\lambda}{P_r}\right)\right\}\left(\Lambda + \frac{\lambda}{P_r}\right),$$

$$a_2 = \frac{R_s(\tau-\lambda)}{P_r(\tau+\lambda} - \frac{3\pi^2}{D_a}\left(\Lambda+\frac{\tau}{P_r}\right) + \frac{1}{D_a^2}\left\{1 - 4\pi^2 D_a\left(\Lambda+\frac{\lambda}{P_r}\right)\right\},$$

$$a_1 = -2\pi^2\left\{\frac{R_s(\tau-\lambda)}{P_r(\tau+\lambda)} + \frac{1}{D_a^2}\right\},$$

$$a_0 = \frac{R_s\pi^2(\tau-\lambda)}{P_r(\tau+\lambda)} \quad \text{and} \quad Y = \alpha_c^2 + \pi^2 .$$

We see that α_c^2 depends not only on D_a and Λ but also on R_s, P_r, τ and λ. As $P_r \to \infty$, Eq.(15) simply reduces to

$$(D_a\Lambda Y^2+1)^2\left(2D_a\Lambda Y^2 + (1-3\pi^2 D_a\Lambda)Y - 2\pi^2\right) = 0 .$$

Since $(D_a\Lambda Y^2+1)^2 \neq 0$,

$$2D_a\Lambda Y^2 + (1-3\pi^2 D_a\Lambda)Y - 2\pi^2 = 0 ,$$

and on simplification we find that this equation is the same as Eq. (12).

Figures 2 and 3 summarise the stability regions in the $R - R_s$ plane for $D_a^{-1} = 100$, $\tau = 0.32$ and $D_a^{-1} = 1000$, $\tau = 0.01$ respectively with $P_r = 7.0$ and $\gamma = 0.2$. In the fourth quadrant, where R is negative and R_s is positive, both gradients are stabilising, and no instability is possible. In the second quadrant all points are unstable above the line defined by Eq. (11), and the instability sets in the direct mode. In the first quadrant ($R_s > 0,\ R > 0$) the instability

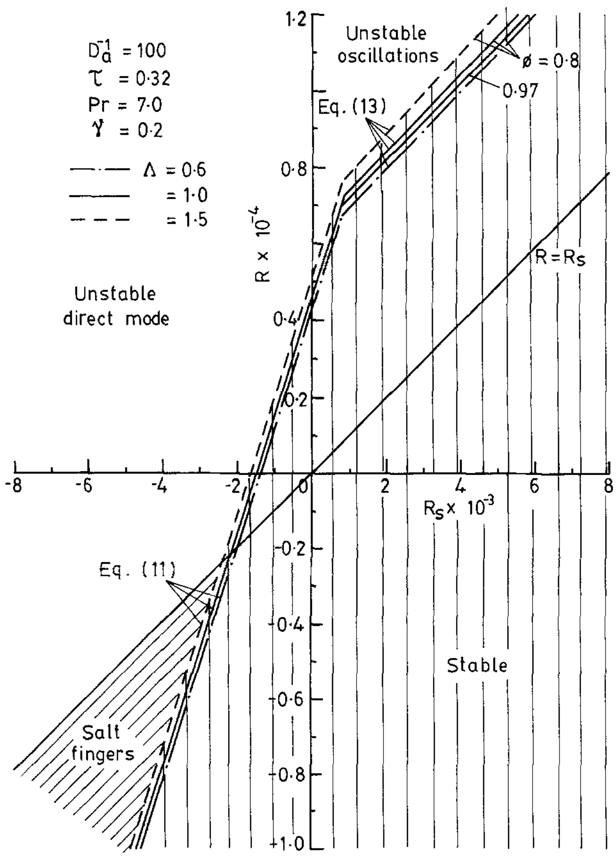

Fig. 2. Stability boundaries for different values of Λ and φ

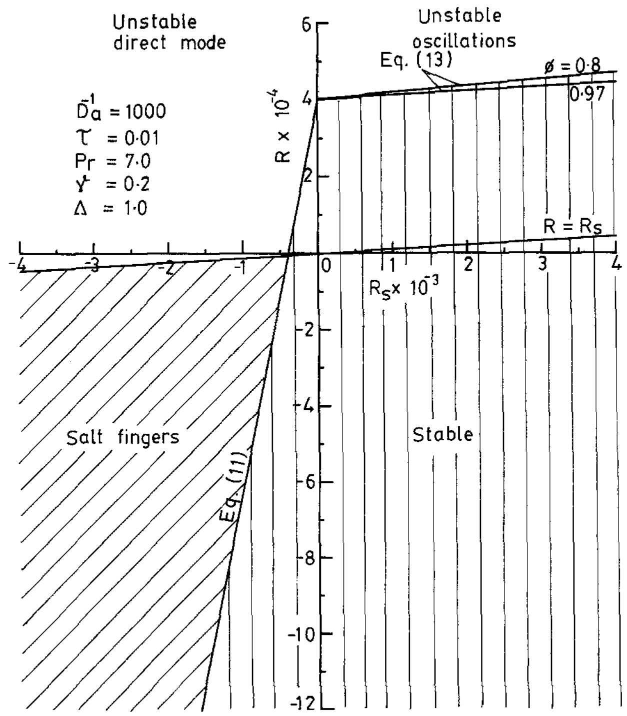

Fig. 3. Stability boundaries for different values of φ

sets in the overstable mode, above the line defined by Eq. (13). At $R_s = R_s^*$ the slope of the $R - R_s$ plot changes, as does the preferred mode of instability. From these figures it is evident that the increase in the value of Λ and decrease in the value of φ is to increase the region of stability. That is, their effect is to delay the onset of convection. The line

$$R = R_s \tag{16}$$

on which $\partial \varrho / \partial z = 0$ is also shown in the figure. Below this line the net density gradient is statically stable. Focussing on the third quadrant, where both R and R_s are negative, one sees a region in which direct mode instability sets in, even though the net density gradient is statically stable. The region extends between the lines defined by Eqs. (11) and (16) and is analogus to the 'finger regime'.

2.4 Transition from oscillatory to direct instability

In the limit $\mathrm{Im}(\sigma) \to 0$, the oscillatory modes with zero frequency can be interpreted as convective modes (Veronis [10]). These occur with $Re\,(\sigma) > 0$, and in some cases the corresponding Rayleigh number, R^{oo} (say) is less than R^d.

To obtain R^{oo}, i.e., at which the transition from oscillatory to direct instability occurs, let us write Eq. (9) as

$$\tilde{\sigma}^3 + (1 + \tilde{\tau} + P_r \tilde{\eta})\,\tilde{\sigma}^2 + \left((\tilde{r}_s - \tilde{r})\,P_r + \tilde{\tau} + P_r(1 + \tilde{\tau})\,\tilde{\eta}\right)\tilde{\sigma} + \left(P_r \tilde{\tau}\tilde{\eta} + (\tilde{r}_s + \tilde{\tau}\tilde{r})\right) = 0\,, \tag{17}$$

where

$$\tilde{\sigma} = \frac{\sigma}{K^2}\,, \qquad \tilde{r} = \frac{\alpha^2 R}{K^6 \lambda}\,, \qquad \tilde{r}_s = \frac{\alpha^2 R_s}{K^6 \lambda^2}\,, \qquad \tilde{\eta} = \frac{\eta}{\lambda}\,, \qquad \tilde{\tau} = \frac{\tau}{\lambda}\,.$$

In general $\tilde{\sigma}$ has three roots with two of them being complex conjugates and corresponding to oscillatory modes which may grow or decay. The limit of zero frequency is given by the vanishing of the discriminant of Eq. (17), i.e., by

$$\left(\left((\tilde{r}_s - \tilde{r})\, P_r + \tilde{\tau} + P_r(1+\tilde{\tau})\,\tilde{\eta}\right) - \frac{1}{3}(1+\tilde{\tau}+P_r\tilde{\eta})^2\right)^3$$

$$+\frac{3}{4}\Bigg[\frac{2}{9}(1+\tilde{\tau}+P_r\tilde{\eta})^3 - (1+\tilde{\tau}+P_r\tilde{\eta})\left((\tilde{r}_s - \tilde{r})\, P_r + \tilde{\tau} + P_r(1+\tilde{\tau})\,\tilde{\eta}\right)$$

$$+3(P_r\tilde{\eta}\tilde{\tau} + \tilde{r}_s - \tilde{\tau}\tilde{r})\Bigg]^2 = 0\,.$$

This is a cubic equation for $\tilde{r}$, and to find R^{oo}, it has to be solved numerically. We note that R^{oo} depends on R_s, τ, λ, P_r, Λ and D_a, and asymptotically $R^{oo} \to R_s/\lambda$ as $R_s \to \infty$.

The foregoing results of the linear theory may be summarised as follows: when $\omega^2 > 0$, Hopf bifurcation first sets in at R^o and there is a transition to overturning convection at R^{oo} and there is no part played by R^d as far as linear solutions are concerned. On the other hand, if $\omega^2 < 0$, a leak instability appears first at R^d and R^{oo} has no physical significance.

2.5 *Subcritical and supercritical bifurcations*

For the case of $\omega^2 < 0$, as R is increased, the static solution loses stability at R^d where there is a bifurcation to a triplet of steady solutions, one of which is now an unstable static solution. The other two are finite amplitude solutions differing only in the signs of A, B and D. The behaviour of the two branches of steady solutions in the neighbourhood of R^d may be investigated in terms of the A-mode by setting

$$R = R^d + R_2{}^d A^2 + 0(A^4)$$

for $A^2 \ll 1$. Substituting this in Eqs. (8.1) – (8.5) it follows that

$$R_2{}^d = \frac{R_s}{\tau} + \frac{K^6}{\alpha^2}\eta - \frac{R_s}{\tau^3} = R^d - \frac{R_s}{\tau^3}\,. \tag{18}$$

This result is identical to that of the full two-dimensional problem and is shown in the Appendix. As $D_a{}^{-1} \to 0$ and $\Lambda = 1$, the above result coincides with that of Da Costa et al. [8] and Nagata and Thomas [11]. The sign of $R_2{}^d$ indicates the directions of bifurcation; supercritical if $R_2{}^d > 0$ and subcritical if $R_2{}^d < 0$. Correspondingly the finite-amplitude solution is said to be stable and unstable, respectively. Thus $R_2{}^d > 0$ if $0 < \tau < 1$ and $0 < R_s < \bar{R}_s = K^6\eta\tau^3/\left(\alpha^2(1-\tau^2)\right)$ or $\tau > 1$, while $R_2{}^d < 0$ if $0 < \tau < 1$ and $R_s > \bar{R}_s$. Also we note that $\bar{R}_s < R_s{}^*$ so that the branch of convective motions bifurcates subcritically as R increases past R^d when $\bar{R}_s < R_s < R_s{}^*$.

For $R_2{}^d < 0$, there exists a minimum Rayleigh number for steady convection, and it can be determined as follows. The system (8) admits a non-trivial steady solution and is given by

$$B = -\frac{A}{A^2+1}\,, \qquad C = \frac{A^2}{A^2+1}\,, \qquad D = -\frac{\tau A}{A^2+\tau^2}\,, \qquad E = \frac{A^2}{A^2+\tau^2}\,,$$

where A satisfies the equation

$$\tilde{\eta}A^4 + \left(\tilde{\eta}(1+\tau^2) - R + R_s\tau\right) A^2 + \tau^2\left(\tilde{\eta} - R + \frac{R_s}{\tau}\right) = 0 \tag{19}$$

or $A = 0$ (pure conduction), with $\tilde{\eta} = \eta K^6/\alpha^2$. The condition that must be satisfied is that the discriminant of Eq. (19) is non-negative. Hence the limiting condition for real A^2 is

$$\left(\tilde{\eta}(1+\tau^2) - R + R_s\tau\right)^2 - 4\tilde{\eta}\tau^2\left(\tilde{\eta} - R + \frac{R_s}{\tau}\right) = 0.$$

The solution for this equation for R is denoted by R^f and is given by

$$R^f = \left(\sqrt{R_s\tau} + \sqrt{\tilde{\eta}(1-\tau^2)}\right)^2. \tag{20}$$

The second solution for R leads to negative values for R^f and is therefore omitted. Equation (20) gives meaningful results provided $R_s > 0$ and $\tau < 1$. We note that $R^f_{\min}$, the minimum value of R^f at which a steady finite amplitude solution can exist, occurs at the same value of $\alpha^2 = \alpha_c{}^2$ at which $R^d_{\min}$ exists. For a single component (i.e., no solute concentration) fluid, we find that $R^f = R^d$ and hence subcritical motions are not possible. To see the possibility of occurring finite amplitude instability, the values of $R^d_{\min}$, $R^o_{\min}$, $R^{oo}_{\min}$ and $R^f_{\min}$ are plotted as functions of R_s, for different values of $D_a{}^{-1}$ and are shown in Fig. 4. From this figure we note that an increase in $D_a{}^{-1}$ is to increase the value of R and thus makes the system more stable. The values of $R^{oo}_{\min} > R^o_{\min}$ so that the oscillatory motions will occur first and $R^{oo}_{\min}$ stands as a correction to $R^d_{\min}$. It is also evident that, although the onset of convection occurs as time periodic motion according to the linear theory, the finite amplitude steady motions can exist for values of the Rayleigh number even smaller than $R^o_{\min}$. Thus once the system becomes unstable, whether it is to infinitesimal perturbations at $R = R^o_{\min}$, or to finite amplitude perturbations at $R < R^o_{\min}$, the developed state of convection will be steady.

Asymptotically, $R^d \to R_s/\tau$, $R^o \to R_s(P_r\eta + \tau)/\lambda(P_r\eta + \lambda)$, $R^{oo} \to R_s/\lambda$, $R^f \to R_s\tau$ as $R_s \to \infty$.

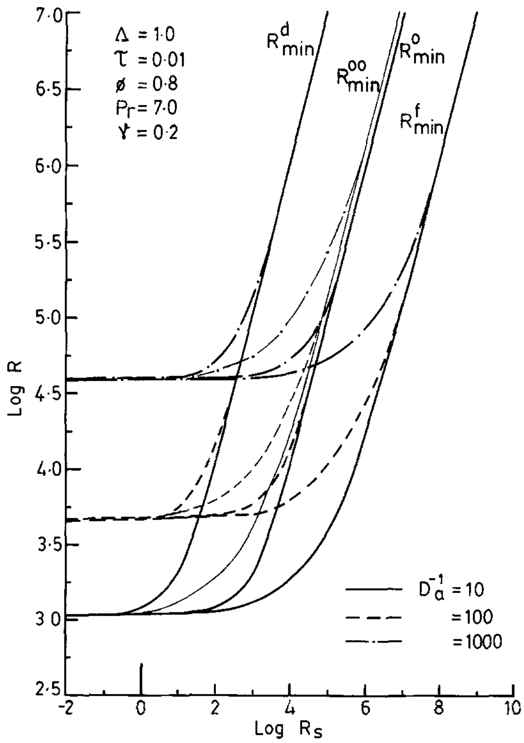

Fig. 4. Curves of $R^d_{\min}$, $R^o_{\min}$, $R^{oo}_{\min}$ and $R^f_{\min}$ as functions of R_s for different values of $D_a{}^{-1}$

2.6 Convective heat and mass transport

The vigour of double diffusive convection can be measured in terms of Nusselt numbers Nu (thermal) and Nu_s (solutal). In the steady state, the vertical heat (or solute concentration) flux is independent of the vertical coordinate, z, and it can be evaluated as $H_T = -\varkappa \langle \partial T / \partial z \rangle_{z=0}$, where the angular brackets correspond to a horizontal average. Since $\partial T / \partial z$ is composed of the constant gradient plus the change in the meanfield, the Nusselt number is calculated as

$$\mathrm{Nu} = \frac{H_T d}{\varkappa \Delta T} = 1 + 2C = 1 + \frac{2}{1 + \frac{1}{A^2}},$$

where A^2 can be evaluated from Eq. (19).

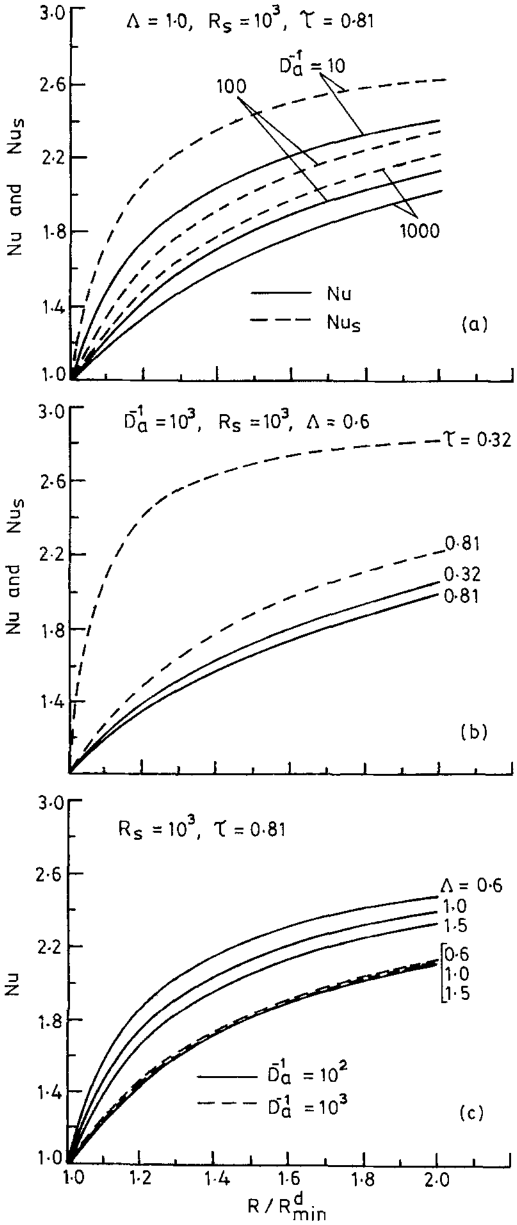

Fig. 5a–c. Variation of Nusselt numbers with Rayleigh number

Similarly, $\mathrm{Nu}_s = 1 + 2E = 1 + \dfrac{2}{1 + \dfrac{\tau^2}{A^2}}$.

At $R = R^d$, $A^2 = 0$ or $A^2 = \dfrac{R_s(1-\tau^2)}{\tilde{\eta}\tau} - \tau^2$.

$A^2 = 0$ corresponds to the conduction state and in this case both Nu and Nu_s will be unity.

At $R = R^f$, $A^2 = \dfrac{\sqrt{R_s(1-\tau^2)}}{\tilde{\eta}} - \tau^2$.

As $R_s \to \infty$, $A \to \infty$, we see that Nu and Nu_s will approximate 3. In Figs. 5a, 5b and 5c the values of Nu and Nu_s vs. $R/R^d_{\min}$ are exhibited in the form of graphs for different values of physical parameters. Figure 5a reveals that at any given value of $R/R^d_{\min}$ the Nusselt number decreases with an increase in ${D_a}^{-1}$ because the resistance offered to the flow by the fluid element in unit volume is sufficiently large so that the system becomes more stable. Figures 5b and 5c depict the effect of τ and Λ on heat and mass transport. From Fig. 5b we note that as τ decreases the values of Nu and Nu_s increase, but the change in the effect of Λ on heat transport is noticeable only for moderate values of D_a (i.e., Brinkman regime). For large values of ${D_a}^{-1}$ the heat transport is almost the same for all the values of Λ considered (see Fig. 5c).

2.7 *Streamlines, isotherms and isohalines*

The stream function ψ is antisymmetric with respect to the line $x = \pi/\alpha$ as it involves a Sine term in x and hence it is sufficient to consider only a half-cell. For a given set of physical parameters, the cell-scale α is fixed, and therefore we confine our attention to the rectangular region $0 \le x \le \pi/\alpha$ and $0 \le z \le 1$. The streamlines drawn corresponding to ${D_a}^{-1} = 100$ and 1000 with two different values of $\Lambda = 1.0$ and 2.5 are shown in Figs. 6a and 6b, respectively. From these figures it is clear that the decrease in the value of Λ is to push the volume transport towards the boundaries of the cell. Also as ψ decreases, the circular stream lines pattern gets deformed into a rectangle and this deformation is more for ${D_a}^{-1} = 100$ as compared to ${D_a}^{-1} = 1000$.

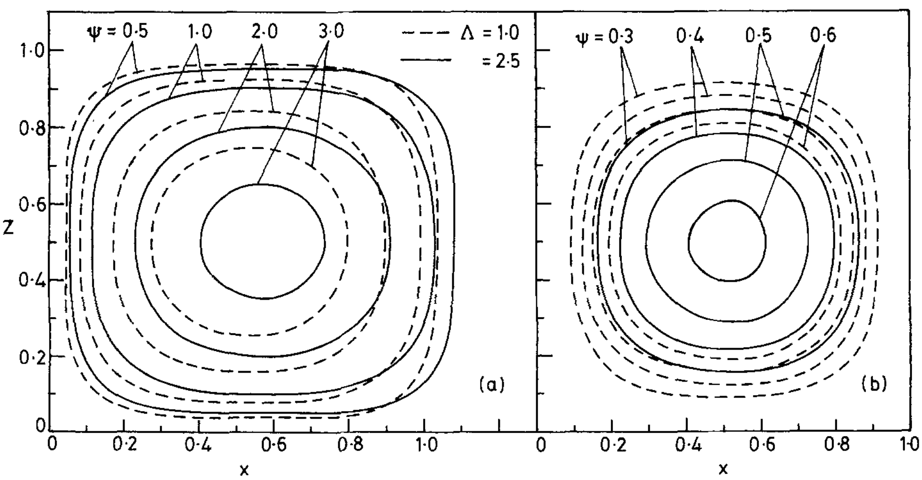

Fig. 6. Streamlines for $R_s = 10^3$, $\tau = 0.32$, $P_r = 1.0$. **a** $R = 10000$, ${D_a}^{-1} = 10^2$, **b** $R = 45000$, ${D_a}^{-1} = 10^3$

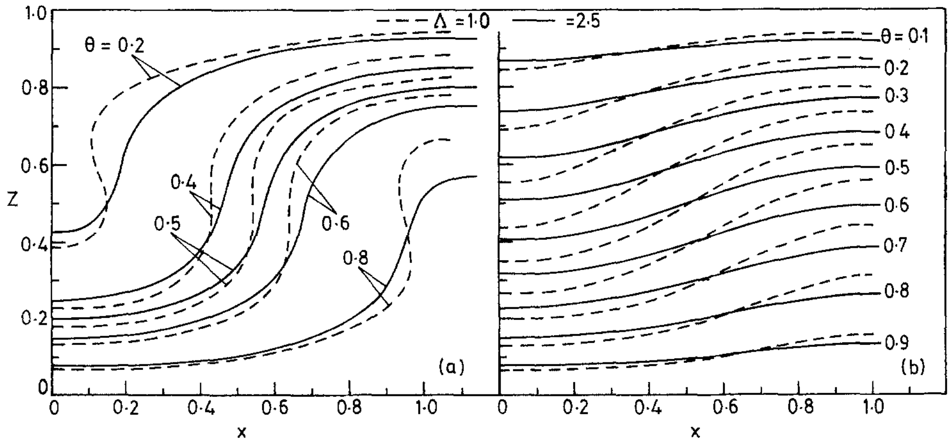

Fig. 7. Isotherms for $R_s = 10^3$, $\tau = 0.32$, $P_r = 1.0$. **a** $R = 10000$, ${D_a}^{-1} = 10^2$, **b** $R = 45000$, ${D_a}^{-1} = 10^3$

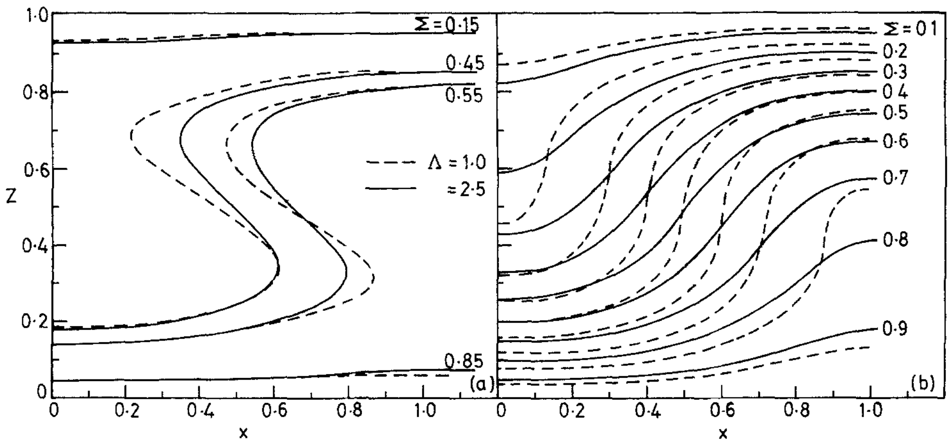

Fig. 8. Isohalines for $R_s = 10^3$, $\tau = 0.32$, $P_r = 1.0$. **a** $R = 10000$, ${D_a}^{-1} = 10^2$, **b** $R = 45000$, ${D_a}^{-1} = 10^3$

The contours of isotherms and isohalines are shown in Figs. 7a, 7b and 8a, 8b, respectively, for two values D_a^{-1} ($= 100$, 1000) and $\Lambda(= 1.0, 2.5)$. From these figures it is evident that isotherms and isohalines in the centre of the cell are more or less vertical (i.e., anvil-shaped) for ${D_a}^{-1} = 100$. But an increase in the value of ${D_a}^{-1}$ and Λ is to inhibit the anvil shaped plumes, and this inhibition is found to be more for isotherms as compared to isohalines. Also these contours are horizontal near the upper and lower boundaries, where conduction is important, and they are flat near $x = 0$ and $x = \pi/\alpha$.

3 Results

The results of the present investigation may be summarised as follows:

(i) Increase in viscosity ratio and decrease in porosity and Darcy number is to delay the onset of convection.

(ii) Hopf bifurcation is possible for a certain choice of physical parameters, and it always occurs at a lower value of the Rayleigh number than the one obtained for simple bifurcation. Also, the condition for the transition from oscillatory to direct instability is obtained.

(iii) Self-adjoint operator technique is used to find the eigenvalues of the problem. The finite amplitude steady motions can exist for a certain choice of physical parameters. That is, subcritical steady convection is possible for values of the Rayleigh number even smaller than $R^o_{\min}$.

(iv) Decrease in diffusivity and viscosity ratios and increase in Darcy number is to increase the heat and mass transfer. Also, increase in viscosity ratio and decrease in Darcy number is to push the volume transport towards the centre of the convective cell and to inhibit the anvil shaped plumes, and this inhibition is more pronounced in isotherms than in isohalines.

Appendix

A.1 Finite – amplitude direct modes

Modified perturbation theory is employed to investigate steady solutions in the neighbourhood of the simple bifurcation at R^d. Accordingly, we expand the dependent variables (i.e., ψ, θ and Σ) and one of the Rayleigh numbers R in terms of a small parameter ε, such that

$$\begin{aligned} \psi &= \varepsilon\psi_1 + \varepsilon^2\psi_2 + \cdots, \\ \theta &= \varepsilon\theta_1 + \varepsilon^2\theta_2 + \cdots, \\ \Sigma &= \varepsilon\Sigma_1 + \varepsilon^2\Sigma_2 + \cdots \end{aligned} \tag{A1}$$

and

$$R = R^d + \varepsilon {R_1}^d + \varepsilon^2 {R_2}^d + \cdots. \tag{A2}$$

At each stage in the expansion, we may define a column vector,

$$\Psi_n = [\psi_n,\ \theta_n,\ \Sigma_n]^t. \tag{A3}$$

Substituting Eq. (A1) and Eq. (A2) into Eqs. (1) – (3) and setting time derivatives to zero then at leading order in ε the equations are linear homogeneous and can be written in the operator form

$$L\Psi_1 = 0, \tag{A4}$$

where L is a self-adjoint differential operator and is given by

$$L = \begin{bmatrix} \dfrac{({D_a}^{-1} - \Lambda\nabla^2)\nabla^2}{R_0} & r^d\dfrac{\partial}{\partial x} & -r_s\dfrac{\partial}{\partial x} \\ -r^d\dfrac{\partial}{\partial x} & r^d\nabla^2 & 0 \\ r_s\dfrac{\partial}{\partial x} & 0 & -r_s\tau\nabla^2 \end{bmatrix}. \tag{A5}$$

Here $r^d = R^d/R_o, r_s = R_s/R_o$ and $R_o = K^6/\alpha^2$.

This is just the two dimensional form of the eigenvalue problem and has been already discussed where we have $r^d = r_s/\tau + \eta$, and the eigenfunction is

$$\Psi_1 = 2\sqrt{2}\left(\frac{K}{\alpha}\right)\begin{bmatrix} \sin\alpha x \sin\pi z \\ \left(\frac{\alpha}{K^2}\right)\cos\alpha x \sin\pi z \\ \left(\frac{\alpha}{K^2}\right)\cos\alpha x \sin\pi z \end{bmatrix}. \tag{A6}$$

The normalisation chosen above is for subsequent convenience. The operator L is self-adjoint, and hence we have the identity

$$\langle \Psi_1{}^T L\Psi_n\rangle = \langle \Psi_n{}^T L\Psi_1\rangle = 0 \tag{A7}$$

for all n. Here the angular brackets denote averages over the domain $0 \le x \le 2\pi/\alpha$ and $0 \le z \le 1$.

To second order in ε, the equations are linear inhomogeneous and are given by

$$L\Psi_2 = \begin{bmatrix} -r_1{}^d \dfrac{\partial\theta_1}{\partial x} + \dfrac{1}{P_r R_o} J(\Psi_1, \nabla^2\Psi_1) \\ -r^d J(\Psi_1, \theta_1) \\ r_s J(\Psi_1, \Sigma_1) \end{bmatrix}. \tag{A8}$$

From Eq. (A6) it follows that $J(\Psi_1, \nabla^2\Psi_1) = 0$, and the solvability condition on the inhomogeneous Eq. (A8) is obtained by applying Eqs. (A7) and (A6). Then it follows that $r_1{}^d = 0$. If we impose the orthogonality condition

$$\langle \Psi_1{}^T \Psi_n\rangle = 0, \qquad (n \neq 1) \tag{A9}$$

then the solution of Eq. (A8) is found to be

$$\Psi_2 = \begin{bmatrix} 1 \\ -\dfrac{1}{\pi}\sin 2\pi z \\ -\dfrac{1}{\tau^3\pi}\sin 2\pi z \end{bmatrix}.$$

Now, at third order, we have

$$L\Psi_3 = \begin{bmatrix} -r_2{}^d \dfrac{\partial\theta_1}{\partial x} \\ -r^d J(\Psi_1, \theta_2) \\ r_s J(\Psi_1, \Sigma_2) \end{bmatrix}. \tag{A10}$$

As before the solvability condition yields, from Eqs. (A7) and (A10),

$$r_2{}^d = r^d - r_s/\tau^3, \qquad \text{i.e.} \qquad R_2{}^d = R^d - R_s/\tau^3,$$

a result which is identical to the one obtained from the truncated system (cf. Eq. (18)).

Acknowledgements

We thank Prof. N. Rudraiah, INSA Senior Scientist, for his valuable discussions. This work was supported by UGC under DSA and COSIST Programmes.

References

[1] Huppert, H. E., Turner, J. S.: Double-diffusive convection. J. Fluid Mech. **106,** 299–329 (1981).
[2] Nield, D. A.: Onset of thermohaline convection in a porous medium. Water Resources Res. **4,** 553–560 (1968).
[3] Rubin, H.: Effect of nonlinear stabilising salinity profiles on thermal convection in a porous medium layer. Water Resources Res. **9,** 211–220 (1973).
[4] Lightfoot, E. N., Taunton, J. W.: Thermohaline instability and saltfingers in a porous medium. Phys. Fluids **15,** 748–753 (1972).
[5] Rudraiah, N., Srimani, P. K., Friedrich, R.: Finite amplitude convection in a two component fluid saturated porous layer. Int. J. Heat Mass Transfer **25,** 715–722 (1982).
[6] Poulikakos, D.: Double diffusive convection in a horizontally sparsely packed porous layer. Int. Comm. Heat Mass Transfer **13,** 587–598 (1986).
[7] Givler, R. C., Altobelli, S. A.: A Determination of the effective viscosity for the Brinkman-Forchheimer flow model. J. Fluid Mech. **258,** 355–370 (1994).
[8] Nield, D. A., Bejan: Convection in porous media. Wien New York: Springer 1991.
[9] Da Costa, L. N., Knobloch, E., Weiss, N. O.: Oscillations in double diffusive convection. J. Fluid Mech. **109,** 25–43 (1981).
[10] Veronis, G.: Effect of stabilising gradient of solute on thermal convection. J. Fluid Mech. **34,** 315–336 (1968).
[11] Nagata, W., Thomas, W. J.: Bifurcation in doubly-diffusive systems 1; Equilibrium solutions. SIAM J. Math. Anal. 91–113 (1986).

Authors' address: I. S. Shivakumara and R. Sumithra, UGC – DSA Centre in Fluid Mechanics, Department of Mathematics, Bangalore University, Bangalore 560 001, India